HHS Public Access

Author manuscript

J Invest Dermatol. Author manuscript; available in PMC 2019 June 11.

Published in final edited form as:

J Invest Dermatol. 2018 February ; 138(2): 423–433. doi:10.1016/j.jid.2017.08.043.

Extracellular and Non-Chaperone Function of Heat Shock Protein —90α Is Required for Skin Wound Healing

Ayesha Bhatia[1], **Kathryn O'Brien**[1], **Jiacong Guo**[1], **Vadim Lincoln**[1], **Chiaki Kajiwara**[2], **Mei Chen**[1], **David T. Woodley**[1], **Heiichiro Udono**[3], and **Wei Li**[1]

[1]Department of Dermatology, USC-Norris Comprehensive Cancer Center, University of Southern California Keck Medical Center, Los Angeles, California, USA

[2]Department of Microbiology and Infectious Diseases,Toho University School of Medicine, Tokyo, Japan

[3]Department of Immunology, Okayama University Graduate School of Medicine, Dentistry and Pharmaceutical Sciences, Okayama, Japan

Abstract

Despite years of effort and investment, there are few topical or systemic medications for skin wounds. Identifying natural drivers of wound healing could facilitate the development of new and effective treatments. When skin is injured, there is a massive increase of heat shock protein (Hsp) 90α inside the wound bed. The precise role for these Hsp90α proteins, however, was unclear. The availability of a unique mouse model that lacked the intracellular ATPase-driven chaperoning, but spared the extracellular fragment-5—supported pro-motility function of Hsp90α allowed us to test specifically the role of the non-chaperone function of Hsp90 α in normal wound closure. We found that the chaperone-defective Hsp90α-Δ mutant mice showed similar wound closure rate as the wild-type Hsp90α mice. We generated recombinant proteins from the mouse cDNAs encoding the Hsp90α-Δ and wild-type Hsp90α. Topical application of Hsp90α-Δ mutant protein promoted wound closure as effectively as the full-length wild-type Hsp90α protein. More importantly, selective inhibition of the extracellular Hsp90α-Δ protein function by a monoclonal antibody targeting the fragment-5 region disrupted normal wound closure in both wild-type Hsp90α and Hsp90α-Δ mice. Thus, this study provides direct support for non-chaperone, extracellular Hsp90α as a potential driver for normal wound closure.

INTRODUCTION

The approximately year-long wound healing process is divided into (i) an inflammatory phase, (ii) a proliferation phase, and (iii) a maturation phase. After a very brief period of the

Correspondence: Wei Li, Department of Dermatology, USC-Norris, Comprehensive Cancer Center, University of Southern California Keck, Medical Center, 1441 Eastlake Avenue, Los Angeles, California 90089, USA. wli@usc.edu.

CONFLICT OF INTEREST

The authors state no conflict of interest.

SUPPLEMENTARY MATERIAL

Supplementary material is linked to the online version of the paper at www.jidonline.org, and at https://doi.org/10.1016/j.jid.2017.08.043.

inflammation phase, the proliferation phase refers to the period of the following few weeks, during which the granulation tissue is generated and serves as the pavement support for epithelial cells at the wound edge to attach and migrate, resulting in resurfacing of the open wound. Therefore, this phase is known as re-epithelialization or wound closure phase. After wound closure, the long-term maturation phase could take months or years to complete. Most previous studies focused mainly on the initial weeks of the inflammation and wound closure phases due to lack of reliable animal models that allow assessment of the year-long phase of wound maturation (Gurtner et al., 2008;Sen et al., 2009; Singer and Clark, 1999).

For a long time, the conventional wisdom has been that growth factors are regarded as the main driving force of wound closure (Martin, 1997;Werner and Grose, 2003) and have been the center of laboratory investigations and clinical trials. Only recombinant platelet-derived growth factor—BB (Regranex/bercaplermin gel;Smith & Nephew, London, UK) received US Food and Drug Administration approval for topical treatment of diabetic skin wounds 20 years ago. The becaplermin gel has a modest efficacy, with an overall 15% improvement of wound closure (Mandracchia et al., 2001; Nagai and Embil, 2002;Wieman et al., 1998). Recent studies provide several possible explanations. First, most growth factors engage selective cell types. For example, among the three different types of cells critical for wound healing—keratinocytes, dermal fibroblasts, and microvas-cular endothelial cells—platelet-derived growth factor—BB can only engage the platelet-derived growth factor receptor—expressing dermal fibroblasts (Cheng et al., 2011). Second, the transforming growth factor—β family cytokines nullify the effectiveness of most growth factors in the wound bed (Bandyopadhyay et al., 2006). Third, pathological conditions, such as hypoxia and hyperglycemia, compromise the effectiveness of growth factors (Cheng et al., 2011;O'Brien et al., 2014). Based on these findings, we speculated that the factors that drive wound closure do not come from the circulation, the main source of growth factors (Li et al., 2012).

Protein purification from conditioned medium of migrating human keratinocytes allowed us to identify the secreted form of heat shock protein (Hsp) 90α as a possible driver of wound closure by promoting cell survival and cell motility (Bhatia et al., 2016;Cheng et al., 2008;Dong et al., 2016; Li et al., 2007). Mechanistically, secreted Hsp90α binds to the subdomain II in the extracellular part of LRP-1 receptor. The NPVY motif in the cytoplasmic tail of LRP-1 connects Hsp90α signaling to the serine-473, but not threonine-308, phosphorylation in protein kinase B (Akt). Akt1 and Akt2 work in concert, rather than individually, to mediate extracellular Hsp90α signaling to cell motility and wound closure (Tsen et al., 2013). Most encouragingly, secreted Hsp90α binds to a common cell surface receptor, LRP-1, present in all three types of skin cells, which is resistant to transforming growth factor—β inhibition and remains fully active under hypoxia and hyperglycemia (Cheng et al., 2008, 2011; Woodley et al., 2009). Topical application of the full-length or the fragment-5 peptide of Hsp90α accelerated closure of excision, burn, and diabetic wounds in rodent and porcine models (Bhatia et al., 2016;Cheng et al., 2011;Jayaprakash et al., 2015; Li et al., 2007;0'Brien et al., 2014).

However, the critical question of whether the secreted, instead of intracellular, Hsp90α is a driver of normal wound closure remained unanswered. In this study, we utilized a unique mouse model that expresses a truncated Hsp90α-Δ protein. The 232-amino acid deletion

from the carboxyl terminus destroyed the ability of Hsp90α-Δ to dimerize and function as an intracellular chaperone (Allan et al., 2006), but Hsp90α-Δ retains the entire fragment-5 fragment (Cheng et al., 2011). Thus, this mouse allows us to focus on the nonchaperone function of Hsp90α during wound closure in the background of the absence of intracellular Hsp90α chaperone. We demonstrate that secreted Hsp90α is required for normal skin wound closure.

RESULTS

Injury induces increased deposition of Hsp90α protein in wound bed

We postulated that the endogenous Hsp90α expression must dramatically increase in response to injury if Hsp90α acts as a driver of wound closure. We tested this hypothesis in more than one preclinical models to ensure that change of Hsp90α expression is independent of any characteristics of wound healing from a specific animal model. In domestic pigs, which have skin and wound healing mechanisms closest to humans, standard skin biopsies were obtained on day 0, 2, 4, and 7 from 1.5 × 1.5-cm full-thickness wounds, as described previously (O'Brien et al., 2014) and probed with a monoclonal antibody against Hsp90α in the absence or presence of an excessive amount of recombinant Hsp90α protein as a specificity control. An antibody against keratins was included as nonspecific IgG control. As shown in Figure 1, the control anti-keratin antibody only labeled the epidermis throughout the 7-day period of wound closure with minimal changes in intensity (Figure 1a, arrows). When duplicate samples were stained with anti-Hsp90α antibody, however, a time-dependent increase of the staining was detected inside the wound bed (Figure 1b). As shown, a low level of Hsp90α was detected around the epidermis on day 0, followed by a modest increase on day 2 in both epidermal and dermal areas. Through the post-wounding days 4 through 7, a dramatic increase in Hsp90α staining throughout the wound bed was detected. Quantitation of the staining is shown as optical density in Figure 1b, insets (Methods). The antibody staining in the wounds was specific to Hsp90α, because the addition of an excessive amount of recombinant Hsp90α blocked the antibody staining (Figure 1b, bottom panel). We then confirmed these finding using the mouse model of this study. As shown in Figure 2a, wounding induced a time-dependent increase of Hsp90α, and this increased staining declined in the dermis area after complete wound closure. The staining is Hsp90α-specific, because the addition of excessive recombinant Hsp90α protein almost completely blocked the staining (Figure 2a, right side panels). Quantitation of the staining is shown as optical density in insets, as mentioned previously. Please note that because the mouse skin (epidermis and dermis) is significantly thinner than the pig skin, it was especially challenging to obtain a whole wound biopsy on day 0. Taken together, these findings prompted us to investigate the role of the increased Hsp90α proteins in wound closure.

A unique Hsp90αΔ-expressing mouse model that allows distinguishing non-chaperone function from chaperone function of Hsp90α in wound closure

The dramatic increase of Hsp90α in the wound bed between post wounding days 4 through 7, could be due to several mechanisms: (i) increased secretion by the resident skin cells in the wound bed, (ii) increased expression of Hsp90α inside the cells in the wound bed; (iii)

increased Hsp90α from inflammatory cells that had migrated into the wound bed, or (iv) some combination of these. We were looking for a mouse model that could allow us to specifically examine the extracellular and non-chaperone function of Hsp90α during wound closure. We made a surprising finding. The following is how it happened. Imai et al. (2011) initially used gene-trapping technology to make a 232-amino acid deletion at the C-terminal region of Hsp90α to destroy its intracellular chaperone function in a transgenic mouse model. In theory, the truncated form of Hsp90α, that is, Hsp90α-Δ, should be expressed. However, the authors did not detect the Hsp90α-Δ mutant at the time and, therefore, reported the mouse as "Hsp90α-K0 mouse" (Imai et al., 2011). When we reanalyzed these mice, we, surprisingly, detected the truncated form of Hsp90α protein, that is, Hsp90α-Δ. The reason Hsp90α-Δ was previously overlooked is unclear. Most importantly, the Hsp90α-Δ mutant is defective for its intracellular chaperone function, but still contains the entire 115—amino acid fragment-5 for its extracellular function to promote wound closure (Cheng et al., 2011). Therefore, this mouse model allows us to test: (i) wound closure rate in the absence of the Hsp90α's intracellular chaperone function and (ii) the role for the non-chaperone Hsp90α-Δ mutant in wound closure. As shown in Figure 3a, Hsp90α-$\Delta^{+/-}$ and Hsp90α-$\Delta^{-/-}$ mice showed little difference in their phenotypes from the wild-type Hsp9α (Hsp90α-wt)$^{+/+}$ lit-termates, as reported previously (Imai et al., 2011). Geno-typing revealed that a 2.0-kb fragment of DNA in the mice$^{+/+}$ was replaced by a 1.4-kb fragment of DNA in the mice$^{-/-}$ (Figure 3b, lane 4 vs. lane 2). Similar results were obtained by reverse transcriptase—PCR analysis of mRNAs from isolated dermal fibroblasts of these mice (Figure 3c, lane 4 vs. lane 2). Then, the total lysates of dermal fibroblasts isolated from each of the three mice were immunoblotted with anti-Hsp90α or Hsp90β antibody (Methods). As shown in Figure 3d, we detected, as expected, slightly increased Hsp90β in the cells from mice$^{-/-}$ (Figure 3d, middle panel, lane 3), consistent with the previous report (Imai et al., 2011). Unexpectedly, when the duplicate membrane was blotted with anti-Hsp90α antibody, we detected a full-length Hsp90 protein in the same cells from the mice$^{-/-}$ (Figure 3d, upper panel, lane 3). We speculated that this protein species (arrow) was due to cross reactivity of the anti-Hsp90α antibody with Hsp90β. To test this theory, we recovered this protein species by anti-Hsp90 antibody immunoprecipitation. The success of the immunoprecipita-tion was confirmed by Western blotting 10% of the total samples with the same anti-Hsp90α antibody used in immunoprecipitation (Figure 3e). The remaining 90% of the immunoprecipitation samples was resolved in SDS-PAGE and stained with Coomassie brilliant blue to visualize the full-length Hsp90 protein species in the cells from mice$^{-/-}$. The protein bands on Coomassie-stained SDS gel that superimposed with those on the Western blot film, as indicated, were excised and subjected to mass spectrometry analysis (Figure 3f). As expected, band #1 contained peptides from both Hsp90α and Hsp90β; band #2 contained peptides only from Hsp90β, and band #3 contained peptides only from Hsp90α. Therefore, the band #3 must represent the Hsp90α-Δ mutant protein because this protein species was undetectable in mice$^{+/+}$ (lane 1), less in mice$^{-/+}$ (lane 2), and abundant in mice$^{-/-}$ (lane 3). The raw mass spectrometry data of the three marked bands are as shown in Supplementary Figure S1 online. Taken together, these results indicate that (i) the mice$^{-/-}$ are not Hsp90α-knockout mice, as reported previously (Imai et al., 2011) and (ii) the mice$^{-/-}$ do not express the full-length Hsp90α, but express the chaperone-defective Hsp90αΔ mutant protein. This was exactly the mouse model we looked for. For the remaining study, therefore, we switched

the terms of mice$^{-/+}$ and mice$^{-/-}$ to “Hsp90a-D mice,” including Hsp90α-Δ$^{-/-}$ and Hsp90α-Δ$^{-/+}$.

Choosing among loose, contained, and splint wounds for wound closure

Because our focus was on re-epithelialization-driven wound closure, we carried out side-by-side comparisons among the three widely used excision wound models. The idea was to select the one that is more akin to wound healing of humans, that is, more re-epithelialization and less contraction. The three types of excision wounds tested were (i) nonrestricted cover-held or “loose” wounds, (ii) adhesive bandage-held or “contained” wounds, and (iii) adhesive bandage-held and edge-sutured or “splinted” wounds. A schematic representation of the three types of wounds is shown in Supplementary Figure S2a online. The three types of day-0 full-thickness excision wounds in mice are shown in Supplementary Figure S2b and they had variable wound closure rates. Among them, the loose wounds first reached complete closure by day 10 (Supplementary Figure S2b, upper panels). The contained wounds achieved complete closure by day 14 (Supplementary Figure S2b, middle panels). The splinted wounds showed the slowest wound closure and achieve closure around day 17 (Supplementary Figure S2b, lower panels). Quantitation of the wound closure data are shown in Supplementary Figure S2c. Hematoxylin and eosin analysis of completely closed contained versus splinted wounds clearly shows a difference in re-epithelialization (Supplementary Figure S2d, lower panel vs. upper panel). We chose the splinted wound model for the rest of study because it offers maximum wound re-epithelialization and the least wound contraction among the three.

The Hsp90α-Δ$^{-/-}$ mutant mice heal wounds just like Hsp90α-wt mice

The unique Hsp90αΔ$^{-/-}$ mouse model allowed us to study the early phase of wound healing, that is, wound closure, in the absence of the intracellular chaperone function of Hsp90a. Full-thickness splinted excision wounds (8 mm × 8 mm) were created on the back of shaved Hsp90α-wt, Hsp90αΔ$^{+/-}$, and Hsp90αΔ$^{-/-}$ mice. The wounds were covered with 5% carboxymethyl cellulose (CMC) cream to prevent dehydration, bandaged to prevent infection, and allowed to undergo a natural healing process. As shown in Figure 4a, there was little difference in the wound closure rate among the three genetic groups of mice. Quantitation of the wound closure data confirmed this (Figure 4b). Similarly, as shown in Figure 4c, wounds from all three genetic groups of mice showed similar accelerated wound closure in response to exogenously added human recombinant Hsp90α protein on day 0. Quantitation of the wound closure data is shown Figure 4d. These results were confirmed by hematoxylin and eosin analysis of the wound biopsies. As shown in Figure 4e, re-epithelialization of the wounds treated with either CMC control (Figure 4e, upper three panels) or topically applied human recombinant Hsp90 protein (Figure 4e, lower three panels) showed there was indistinguishable difference among the three genetically distinct groups of mice. Based on these findings, we concluded that the intracellular chaperone function of Hsp90α is unessential for normal wound closure.

Recombinant Hsp90α-Δ protein is as effective as full-length Hsp90α in promoting normal wound closure

The next critical question was what makes the wounds of Hsp90α-$\Delta^{-/-}$ mice heal normally or whether the truncated Hsp90α-Δ protein plays any role in normal wound closure. To address this question, we tested whether Hsp90α-Δ mutant protein can act like the full-length Hsp90α protein to promote cell motility in vitro and wound closure in mice. We isolated the full-length Hsp90α and the Hsp90α-Δ mutant cDNAs from the Hsp90α-wt and Hsp90α-$\Delta^{-/-}$ mice and cloned them into the pET15b inducible system in BL-21 bacteria for protein production (Methods). Fast protein liquid chromatography—purified Hsp90α-wt and Hsp90α-Δ proteins are shown in Figure 5a, with known amounts of BSA included as controls for the relative amounts of proteins. As shown in Figure 5b, Hsp90α-wt and Hsp90α-Δ proteins were functionally indistinguishable in promoting primary mouse dermal fibroblast migration by the colloidal gold migration assay (Methods), which we chose to measure and quantify individual cell motility by computer-assisted calculations (Methods). In comparison, the “scratch” and transwell assays are less quantitative for measurement of a purified protein, such as recombinant Hsp90α. The observed variations in induced migration by Hsp90α-wt (Figure 5b, bars 4—6) and Hsp90α-Δ (Figure 5b, bars 7—9) were statistically insignificant. Serum and BSA stimulations were included as positive and negative controls, respectively.

When these proteins were topically applied (only once on day 0) to mouse wounds, as shown in Figure 5c, we found that both Hsp90α-wt (middle panels) and Hsp90α-Δ (bottom panels) proteins accelerated wound closure equally in comparison to the vehicle control (upper panels). Quantitation of data is shown in Figure 5d. The strongest wound closure-promoting effect for both proteins occurred around day 7, consistent with what we have reported previously (Cheng et al., 2011;O’Brien et al., 2014). These findings suggest that the endogenous Hsp90α-Δ protein, likely via its secreted form, was responsible for keeping wound closure as normal in Hsp90α-$\Delta^{-/-}$ mice as the Hsp90α-wt mice.

Extracellular Hsp90α-Δ is required for normal wound closure

The ultimate question regarding drivers of wound closure is whether selective inhibition of the extracellular function of Hsp90α-Δ disrupts normal wound closure. To directly test this hypothesis in the Hsp90α-$\Delta^{-/-}$ mice, we developed a monoclonal antibody, IG6-D7, that binds to the fragment-5 region of Hsp90α via epitope, TKPIWTRNP, and neutralizes the function of secreted Hsp90α or Hsp90α-Δ (Zou et al., 2017). The fragment-5 region in Hsp90α is schematically shown in Figure 6a (Cheng et al., 2011, O’Brien et al., 2014). Because IgG molecules are cell membrane—impermeable, 1G6-D7 should only neutralize the action of the secreted Hsp90α-Δ. As shown in Figure 6b, 1G6-D7 or control IgG was mixed with CMC and topically applied to the wounds on day 0. In the Hsp90α-wt mice, IgG control-treated wounds achieved complete closure at the expected time of day 10 (Figure 6b, upper first row). Interestingly, the addition of 1G6-D7 significantly delayed the time of wound closure (Figure 6b, second row). More intriguingly, in the Hsp90α-$\Delta^{-/-}$ mice, 1G6-D7—treated wounds also exhibited a significantly slowed wound closure (Figure 6b, bottom row). In contrast, the IgG control-treated wounds in these mice healed just like those from the Hsp90α-wt mice (Figure 6b, third row). Quantitation of the wound healing images, as

shown in Figure 6c, confirmed the inhibitory effect by 1G6-D7. Furthermore, we used hematoxylin and eosin staining to visualize the newly re-epithelialized epidermis of IgG-treated or 1G6-D7—treated day 7 wounds in Hsp90α-$\Delta^{-/-}$ mice. As shown in Figure 6d, wound re-epithelialization is dramatically inhibited in 1G6-D7—treated wounds (lower panel), in comparison to IgG-treated wounds (upper panel). Close-up insets show where the newly epithelialized epidermis ended under each of the two conditions (Figure 6d, inserted upper and lower panels). 1G6-D7 also binds, with much less affinity, to secreted Hsp90β than secreted Hsp90a (Zou et al., 2017), but secreted Hsp90β does not have any pro-motility and wound healing—promoting functions (Cheng et al., 2008;Cheng et al., 2011). Therefore, the inhibition of wound closure must be due to neutralization of the extracellularly located Hsp90α-Δ by 1G6-D7. In conclusion, using the unique mouse model of the Hsp90α-$\Delta^{-/-}$ mice and availability of the mAb 1G6-D7, we have demonstrated that the prosurvival and pro-motility functions of secreted Hsp90α, instead of its intracellular chaperone function, are required for normal wound closure.

DISCUSSION

Results of the current study provide key evidence in vivo that the extracellular/secreted, but not the intracellular, Hsp90α is required for normal wound closure. The two critical findings by this study are: (i) topical addition of mouse recombinant Hsp90α-Δ mutant protein was as effective as its full-length Hsp90α counterpart in accelerating wound closure and (ii) inhibition of the secreted Hsp90α-Δ function by a monoclonal antibody inhibitor resulted in significantly delayed wound closure. The latter finding in particular suggests that secreted Hsp90α may play a driver's role in wound closure. This study directly challenges the conventional wisdom that the evolutionarily conserved function for the Hsp90 family proteins is to act as chaperones to stabilize and support the functions of many important signaling pathways, although this historic understanding of Hsp90 family proteins still holds for Hsp90β. While both Hsp90β-knockout mice and cell lines die (Voss et al., 2000; Zou et al., 2017), neither Hsp90α-knockout cells nor Hsp90α chaperone-defective mice (note: they were initially reported as knockout mice) show little phenotypic abnormalities (Grad et al., 2010; Imai et al., 2011; Zou et al., 201 7). By blocking secreted Hsp90α function in wounds with antibodies, Song and Luo (2010) reported a similar finding using a nude mouse model. We have previously postulated that the main physiological function of Hsp90α is tissue repair by its secreted form (Li et al., 2012). Hsp90α is stored in abundance within all the skin cells and is imminently ready for secretion into the extracellular space under the stress of tissue injury and hypoxia. The current study provides a critical support for topically applied recombinant Hsp90α protein as a new wound closure agent for both normal and chronic wounds.

MATERIALS AND METHODS

Animal models

Domestic pigs were housed and used for experiments as described previously (O'Brien et al., 2014). To set up the Hsp90α-$\Delta^{-/-}$ mouse model, heterozygous mouse embryos (frozen at two-cell stage) were obtained from the laboratory of Heiichiro Udono (RIKEN, Saitama,

Japan). The embryos were re-derived at the University of Southern California transgenic core using pseudo-pregnant mice. Both male and female mice of 8—10 weeks old were used for wound closure studies (see additional details for antibodies and protocols in Supplementary Materials online).

Reverse transcriptase—PCR cDNA cloning into pET15b system and protein production

Total RNA was isolated from cultured mouse fibroblasts using TRIzol reagent (Invitrogen, Carlsbad, CA). Reverse transcriptase—PCR was performed using the One Step RT-PCR kit (Qiagen, Hilden, Germany) according to manufacturer's instructions. Primers used for the mouse Hsp90α gene were: (forward) 5'-TAGGCTCTGGATA AATCCGTTACGAGAGC-3' and (reverse) 5'-GATGTGTCGTCATC TCCTTCCAGGGGAG-3'). Verified reverse transcriptase—PCR products (cDNAs) were used as the templates for PCR cloning with primers containing a BamHI site at both ends. The secondary PCR products were subjected to BamHI digestions, gel-purified, and ligated into BamHI-opended pET15b vector for protein production.

Production and fast protein liquid chromatography purification of recombinant Hsp90α proteins were carried out as described previously (Cheng et al., 2008, Zou et al, 2017). All animal experiments were carried out according to approved protocols (for mice and pigs) by the University of Southern California Institutional Animal Use Committee.

Wound closure analysis

Full-thickness, 8-mm wounds were created using punch biopsy and surgical scissors (see detailed protocols in Supplementary Material). Circular silicone splints with an outer diameter of 25.4 mm and inner diameter of 8 mm were prepared by cutting, placed on top of the wound, and adhered to skin using Krazy glue (Elmer's Products, Westerville, OH). The splints were then sutured into the skin at four coordinates surrounding the wound using nylon sutures (Ethicon, Somerville, NJ). For topical treatments, recombinant Hsp90α protein (300 μg per wound)was mixed in 1:1 ratio with 15% sterile CMC in final volume of 100 μl volume. The CMC alone and CMC with Hsp90α proteins were topically applied on wounds in triplicate in three mice. Wounds were covered with Tegaderm film (3M, Maplewood, Minnesota) to prevent desiccation and infection for duration of the experiment. Mice were wrapped around their torso with a self-adherent bandage (3M). Digital photographs were taken individually of the wounds with a metric ruler next to them on the indicated days from a fixed distance by a preset tripod. Biopsies were collected on indicated days and stored in 10% paraffin for sectioning. Photographs of 15 randomly selected images per condition were examined using planimetric measurements for objective evaluation for wound closure rates. The area of an open wound was calculated as height (cm) × width (cm) to give rise to cm2 of the wound. Means of triplicate wounds were used for the presentation. The area of an open wound on a given day was measured and compared to the area of the wound on day 0 from the same animal, using the software AlphaEase FC, version 4.1.0 (Alpha Innotech Corporation, Miami, FL), as described previously (Cheng et al., 2011; Tsen et al., 2013).

Histology and immunohistochemistry

Wedged biopsies measuring 1 cm × 1 cm were taken on the indicated days for skin wounds. The tissue samples were fixed in 10% formalin (VWR, Randor, PA) and placed in paraffin blocks for sectioning by the University of Southern California Pathology Core (see detailed sample selections an measurements in Supplementary Material), as we reported previously (Cheng et al., 2011). To semi-quantitate the staining, we used Gabriel Landini's "colour deconvolution" plugin for ImageJ analysis. Using the Image > Color > Colour Deconvolution, H DAB as vector and Color 2 as DAB image, measurements were carried out to convert intensity to optical density (optical density = log (max intensity / mean intensity, where max intensity = 255 for 80 bit images) (Ruifrok and Johnston, 2001).

Statistical analyses

Data on animal wound healing were based on three independent experiments. Data are presented as mean ± standard deviation. Statistical significance for comparisons was determined by twotailed Student *t* test. *P* values ≤0.05 were considered statistically significant (Cheng et al., 2011).

Supplementary Material

Refer to Web version on PubMed Central for supplementary material.

ACKNOWLEDGMENTS

We thank the University of Southern California Pathology Core for assistance of histological analyses and the Proteomics Core (Ebrahim Zandi) for mass spectrometry analysis. This study is supported by National Institutes of Health grants GM066193 and GM067100 (to WL), AR46538 (to DTW), AR33625 (MC and DTW), and Veterans Affairs Merit Award (to DTW).

Abbreviations:

Akt	protein kinase B
CMC	carboxymethyl cellulose
Hsp	heat shock protein
wt	wild type

REFERENCES

Allan RK, Mok D, Ward BK, Ratajczak T. Modulation of chaperone function and co-chaperone interaction by novobiocin in the C-terminal domain of Hsp90: evidence that coumarin antibiotics disrupt Hsp90 dimerization. J Biol Chem 2006;281:7161–71. [PubMed: 16421106]

Bandyopadhyay B, Fan J, Guan S, Li Y, Chen M, Woodley DT, et al. A "traffic control" role for TGFbeta3: orchestrating dermal and epidermal cell motility during wound healing. J Cell Biol 2006;172:1093–105. [PubMed: 16549496]

Bhatia A, O'Brien K, Chen M, Wong A, Garner W, Woodley DT, et al. Dual therapeutic functions of F-5 fragment in burn wounds: preventing wound progression and promoting wound healing in pigs. Mol Ther 2016;3: 16041.

Cheng CF, Fan J, Fedesco M, Guan S, Li Y, Bandyopadhyay B, et al. Transforming growth factor alpha (TGFalpha)-stimulated secretion of HSP90al-pha: using the receptor LRP-1/CD91 to promote

human skin cell migration against a TGFbeta-rich environment during wound healing. Mol Cell Biol 2008;28:3344–58. [PubMed: 18332123]

Cheng CF, Sahu D, Tsen F, Zhao Z, Fan J, Kim R, et al. A fragment of secreted Hsp90alpha carries properties that enable it to accelerate effectively both acute and diabetic wound healing in mice. J Clin Invest 2011;121: 4348–61. [PubMed: 22019588]

Dong H, Zou M, Bhatia A, Jayaprakash P, Hofman F, Ying Q, et al. Breast cancer MDA-MB-231 cells use secreted heat shock protein-90alpha (Hsp90α) to survive a hostile hypoxic environment. Sci Rep 2016;6:20605. [PubMed: 26846992]

Grad I, Cederroth CR, Walicki J, Grey C, Barluenga S, Winssinger N, et al. The molecular chaperone Hsp90α is required for meiotic progression of spermatocytes beyond pachytene in the mouse. PLoS One 2010;5:e15770.

Gurtner GC, Werner S, Barrandon Y, Longaker MT. Wound repair and regeneration. Nature 2008;453:314–21. [PubMed: 18480812]

Imai T, Kato Y, Kajiwara C, Mizukami S, Ishige I, Ichiyanagi T, et al. Heat shock protein 90 (HSP90) contributes to cytosolic translocation of extracellular antigen for cross-presentation by dendritic cells. Proc Natl Acad Sci 2011;108:16363–8. [PubMed: 21930907]

Jayaprakash P, Dong H, Zou M, Bhatia A, O'Brien K, Chen M, et al. Hsp90α and Hsp90β together operate a hypoxia and nutrient paucity stress-response mechanism during wound healing. J Cell Sci 2015;128:1475–80. [PubMed: 25736295]

Li W, Li Y, Guan S, Fan J, Cheng CF, Bright AM, et al. Extracellular heat shock protein-90alpha: linking hypoxia to skin cell motility and wound healing. EMBOJ 2007;26:1221–33.

Li W, Sahu D, Tsen F. Secreted heat shock protein-90 (Hsp90) in wound healing and cancer. Biochim Biophys Acta 2012;1823:730–41. [PubMed: 21982864]

Mandracchia VJ, Sanders SM, Frerichs JA. The use of becaplermin (rhPDGF-BB) gel for chronic nonhealing ulcers. A retrospective analysis. Clin Podiatr Med Surg 2001;18:189–209, viii. [PubMed: 11344978]

Martin P Wound healing—aiming for perfect skin regeneration. Science 1997;276:75–81. [PubMed: 9082989]

Nagai MK, Embil JM. Becaplermin: recombinant platelet derived growth factor, a new treatment for healing diabetic foot ulcers. Expert Opin Biol Ther 2002;2:211–8. [PubMed: 11849120]

O'Brien K, Bhatia A, Tsen F, Chen M, Wong AK, Woodley DT, et al. Identification of the critical therapeutic entity in secreted Hsp90α that promotes wound healing in newly re-standardized healthy and diabetic pig models. PLoS One 2014;9:e113956.

Ruifrok AC, Johnston DA. Quantification of histochemical staining by color deconvolution. Anal Quant Cytol Histol 2001;23:291–9. [PubMed: 11531144]

Sen CK, Gordillo GM, Roy S, Kirsner R, Lambert L, Hunt TK, et al. Human skin wounds: a major and snowballing threat to public health and the economy. Wound Repair Regen 2009;17:763–71. [PubMed: 19903300]

Singer A, Clark RA. Cutaneous wound healing. N Engl J Med 1999;341: 738–46. [PubMed: 10471461]

Song X, Luo Y. The regulatory mechanism of Hsp90alpha secretion from endothelial cells and its role in angiogenesis during wound healing. Biochem Biophys Res Commun 2010;398:1 11–7.

Tsen F, Bhatia A, O'Brien K, Cheng C-F, Chen M, Hay N, et al. Extracellular heat shock protein 90 signals through subdomain II and the NPVY motif of LRP-1 receptor to Akt1 and Akt2: a circuit essential for promoting skin cell migration in vitro and wound healing in vivo. Mol Cell Biol 2013;33: 4947–59. [PubMed: 24126057]

Werner S, Grose R. Regulation of wound healing by growth factors and cytokines. Physiol Rev 2003;83:835–70. [PubMed: 12843410]

Wieman TJ, Smiell JM, Su Y. Efficacy and safety of a topical gel formulation of recombinant human platelet-derived growth factor-BB (becaplermin) in patients with chronic neuropathic diabetic ulcers. A phase III randomized placebo-controlled double-blind study. Diabetes Care 1998;21:822–7. [PubMed: 9589248]

Woodley DT, Fan J, Cheng CF, Li Y, Chen M, Bu G, et al. Participation of the lipoprotein receptor LRP1 in hypoxia-HSP90alpha autocrine signaling to promote keratinocyte migration. J Cell Sci 2009;122:1495–8. [PubMed: 19383717]

Zou M, Bhatia A, Dong H, Jayaprakash P, Guo J, Sahu D, et al. Evolutionarily conserved dual lysine motif determines the non-chaperone function of secreted Hsp90alpha in tumor progression. Oncogene 2017;36:2160–71. [PubMed: 27721406]

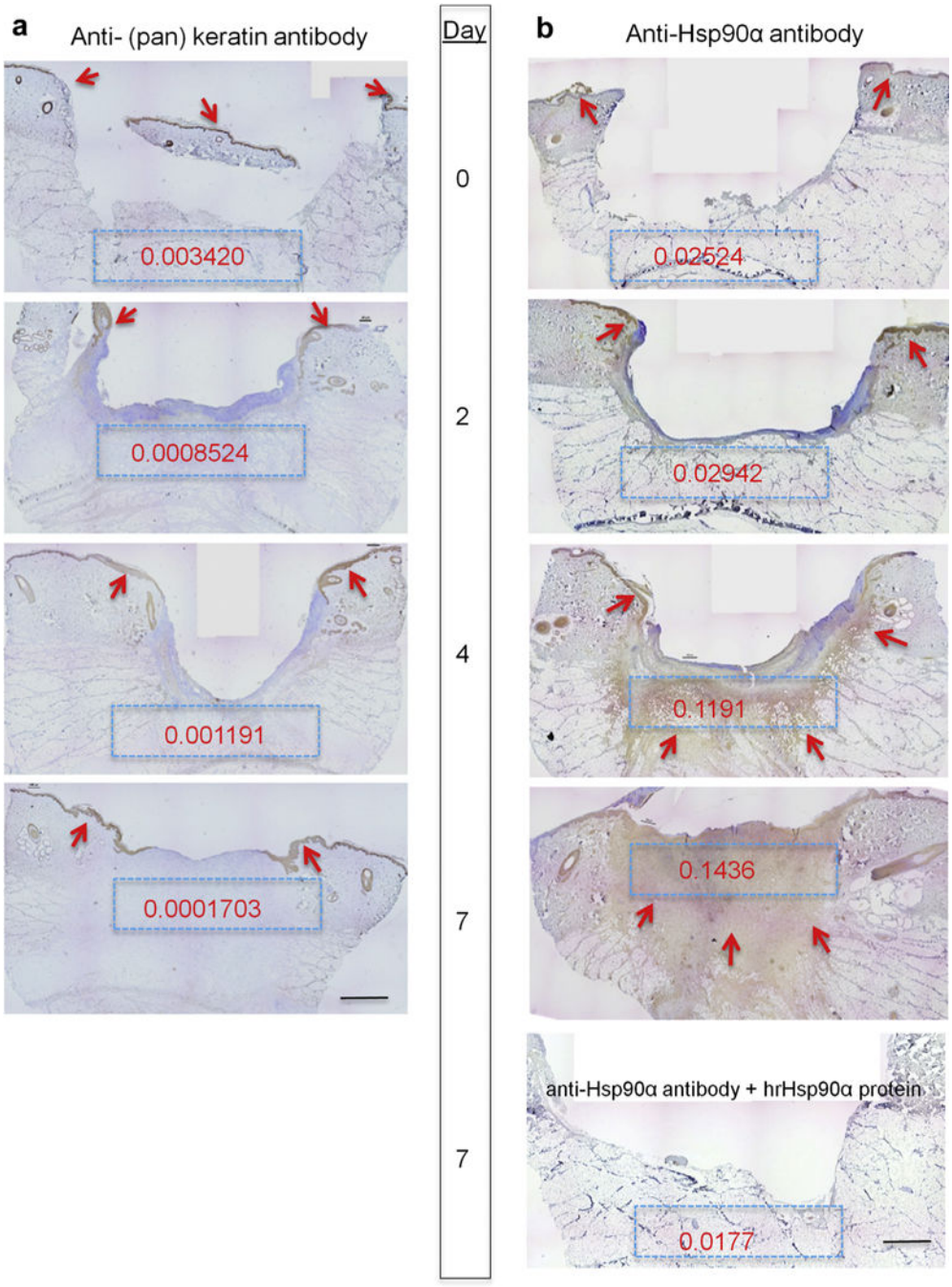

Figure 1. Massive deposition of Hsp90α protein in wound bed following skin injury in pigs.

Nine 1.5 cm × 1.5 cm full-thickness excision wounds were created on the torso side of a pig with 4 cm between the wounds. Wedge biopsies of the entire wounds were taken on the indicated days. Sections of the wounds were subjected to immunohistochemical analysis with (a) anti-(pan) keratin antibody or anti-Hsp90α antibody (1 μg/ml) in the presence or absence of an excessive amount of human recombinant Hsp90α protein (10 μg/ml). The representative images of indicted days are presented. The red arrows point out the locations of the specific antibody staining (brown). To quantitate the staining in each of the blue

boxes, Gabriel Landini's "color deconvolution" and ImageJ analysis were used and the intensity readings were converted to optical density (Methods). Scale bar =2.0 mm. Hsp, heat shock protein.

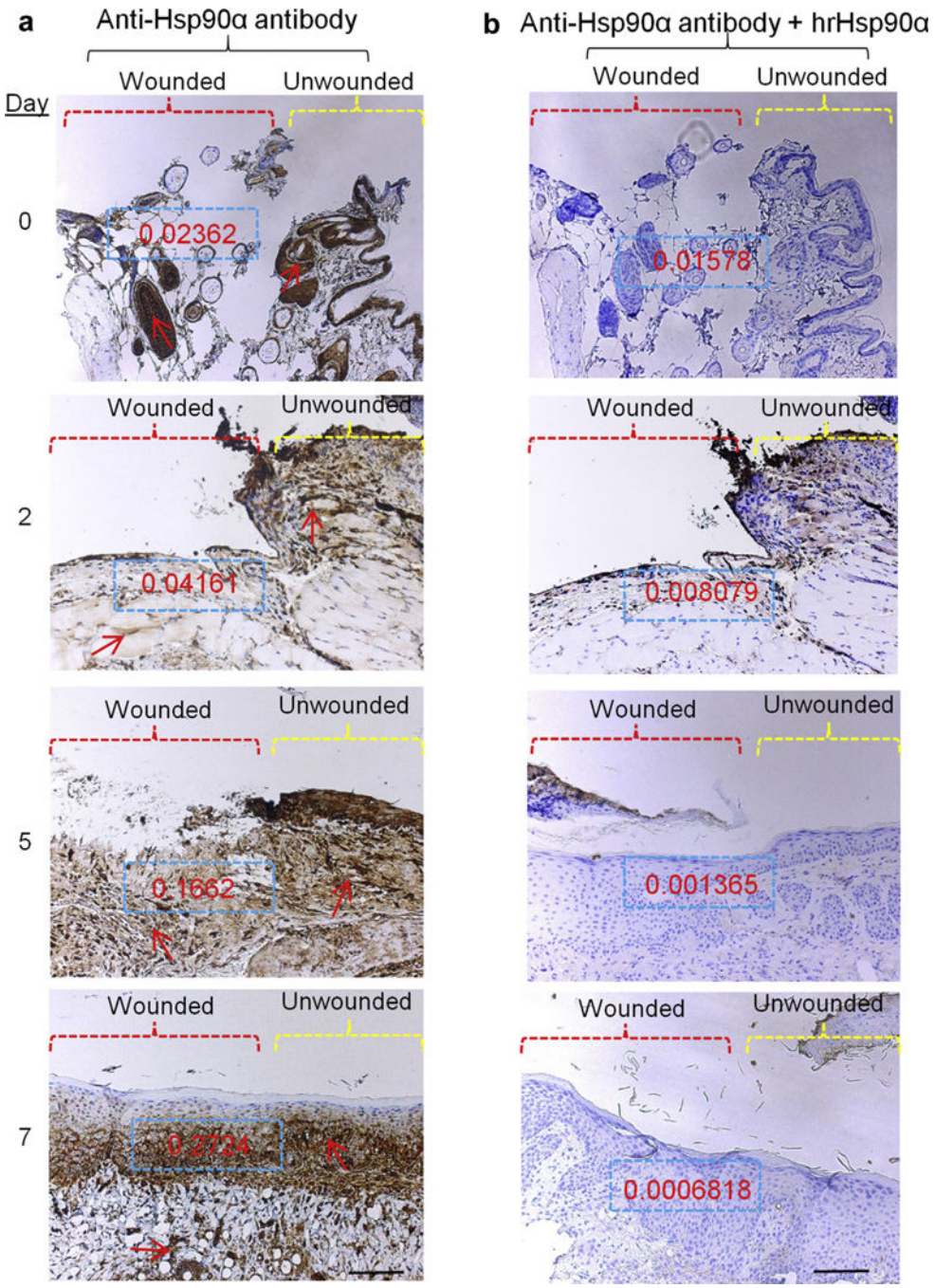

Figure 2. Massively increased Hsp90α in wound bed following skin injury in mice.

Nine 0.8 cm × 0.8 cm full-thickness excision wounds were created on the back of the mice.The wounds were monitored every 24 hours and wedge biopsies of partial (day 0 in particular) or entire wounds were taken on indicated days. Sections of the wounds were subjected to immunohistochemical analyses, exactly as described in Figure 1. These data represent a consensus from multiple and noncontinuous sections of skin specimens. Scale bar = 1.5 mm.Hsp, heat shock protein.

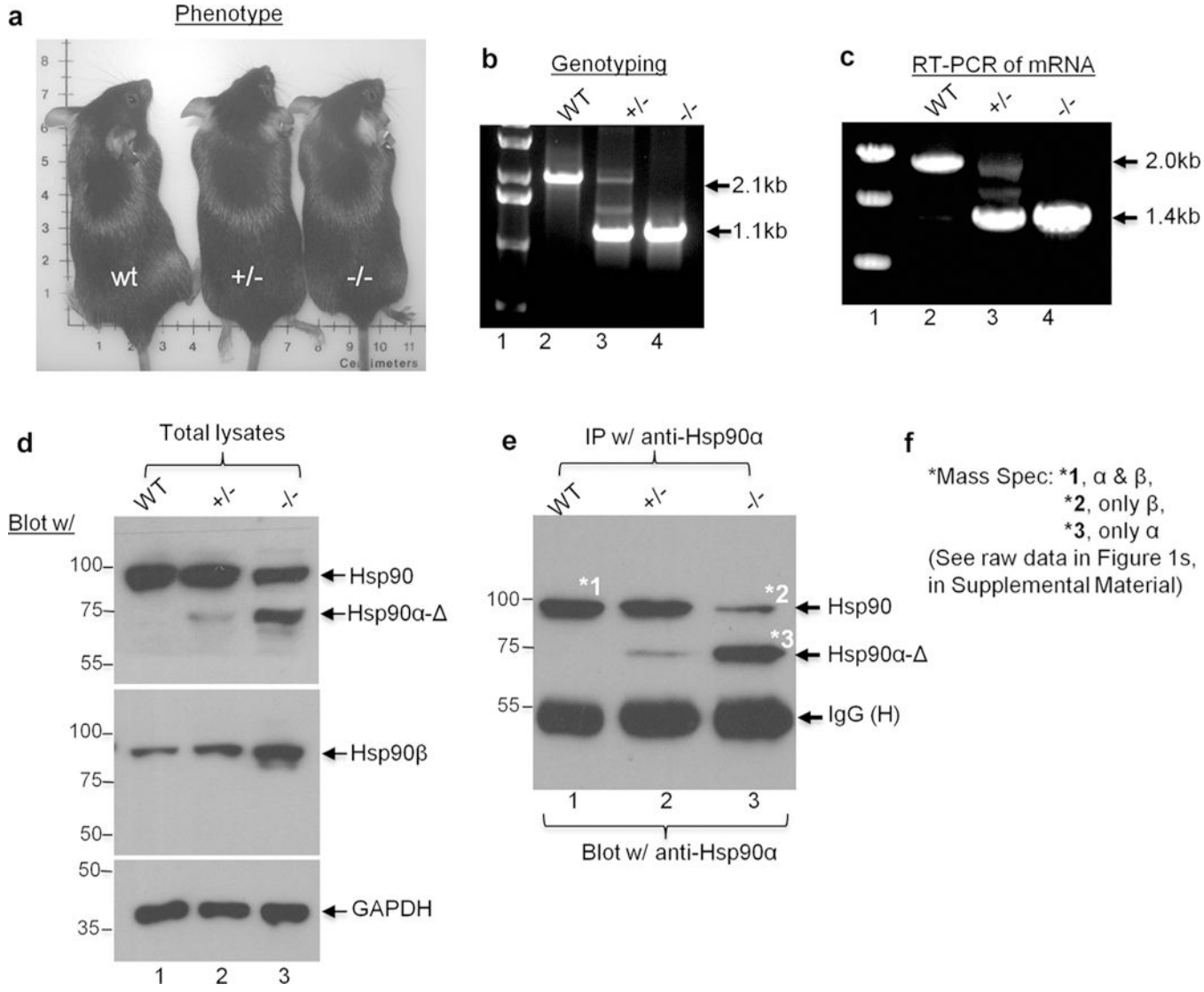

Figure 3. Unique Hsp90α-Δ mouse model to distinguish chaperone and non-chaperone function of Hsp90α for wound closure.

(**a**) The phenotypes of wt, $\Delta^{+/-}$, and $\Delta^{-/-}$ mice are indistinguishable. (**b**) Genotyping data using mouse tail DNAs. (**c**) Reverse transcriptase—PCR analysis of mRNAs isolated from the dermal fibroblasts derived from the indicated mouse skin using the same primers as genotyping. (**d**) Western blots of the total lysates of the cells from wt, $\Delta^{+/-}$, and $\Delta^{-/-}$ mice with indicated antibodies. (**e**) Immunoprecipitation with the indicated anti-Hsp90α or anti-Hsp90β antibodies (Methods). The samples were divided into 10% and 90% two portions, subjected to duplicate SDS-PAGE and subjected to Western blotting with indicated antibodies or stained with Coomassie blue (for mass spectrometry analysis), respectively. (**f**) Three marked bands in (**e**) were excised and subjected to mass spectrometry analysis. Results of the mass spectrometry are summarized as shown. Hsp, heat shock protein; wt, wild type.

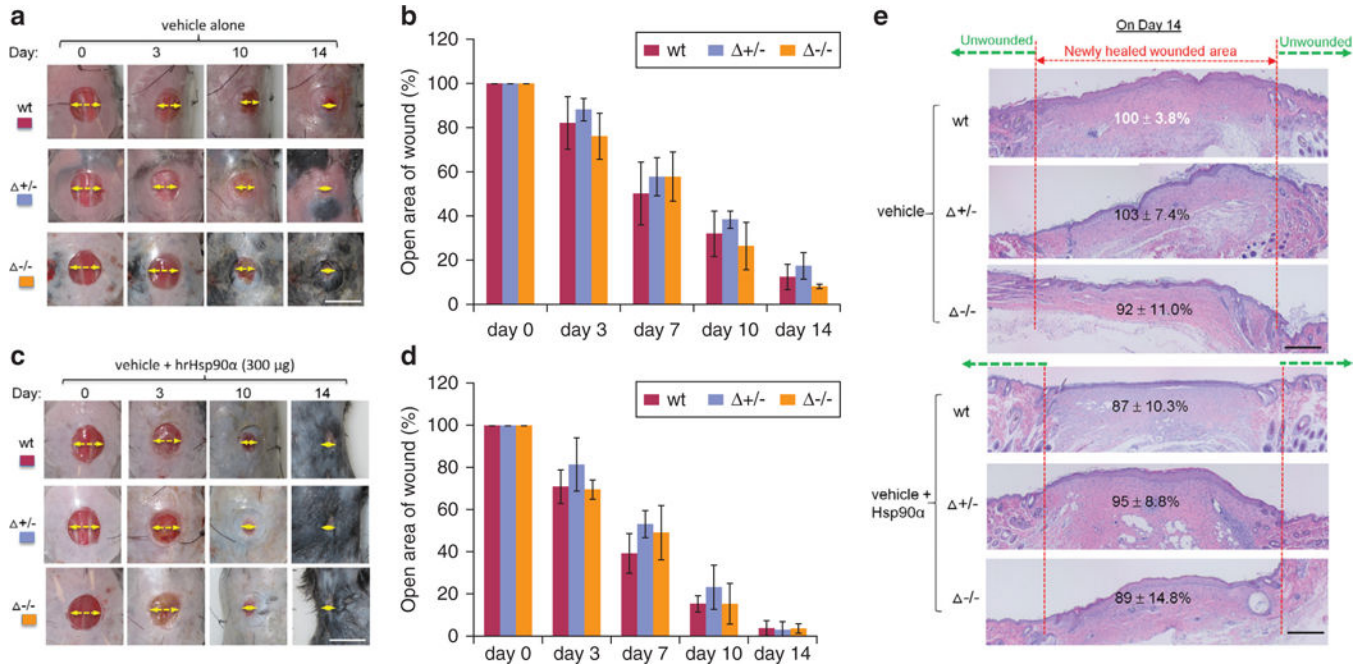

Figure 4. Hsp90α-Δ$^{-/-}$ mice heal wounds as normally as the Hsp90α-wt mice.

(**a**) Images of splinted and untreated wounds undergoing the healing process in three mice over time (n = 3). Yellow arrows indicate the distance of the unhealed part of a wound. (b) Quantitation of the wound closure data shown in (**a**). (**c**) Images of similar splinted wounds with topical recombinant Hsp90α protein treatment in three types of mice over time (n = 3). (**d**) Quantitation of the wound closure data as shown in (**c**). Wounds in triplicates were photographed on an indicated day and analyzed for open wound areas in comparison to their corresponding day-0 wounds as 100%. (**e**) Wedge biopsies on day-14 wounds were subjected to hematoxylin and eosin staining to identify the distance of the newly re-epithelialized epidermis from the edge of unwounded skin. Scale bar for (**a—d**) = 1.0 cm and for (**e**) = 1 mm. Hsp, heat shock protein; wt, wild type.

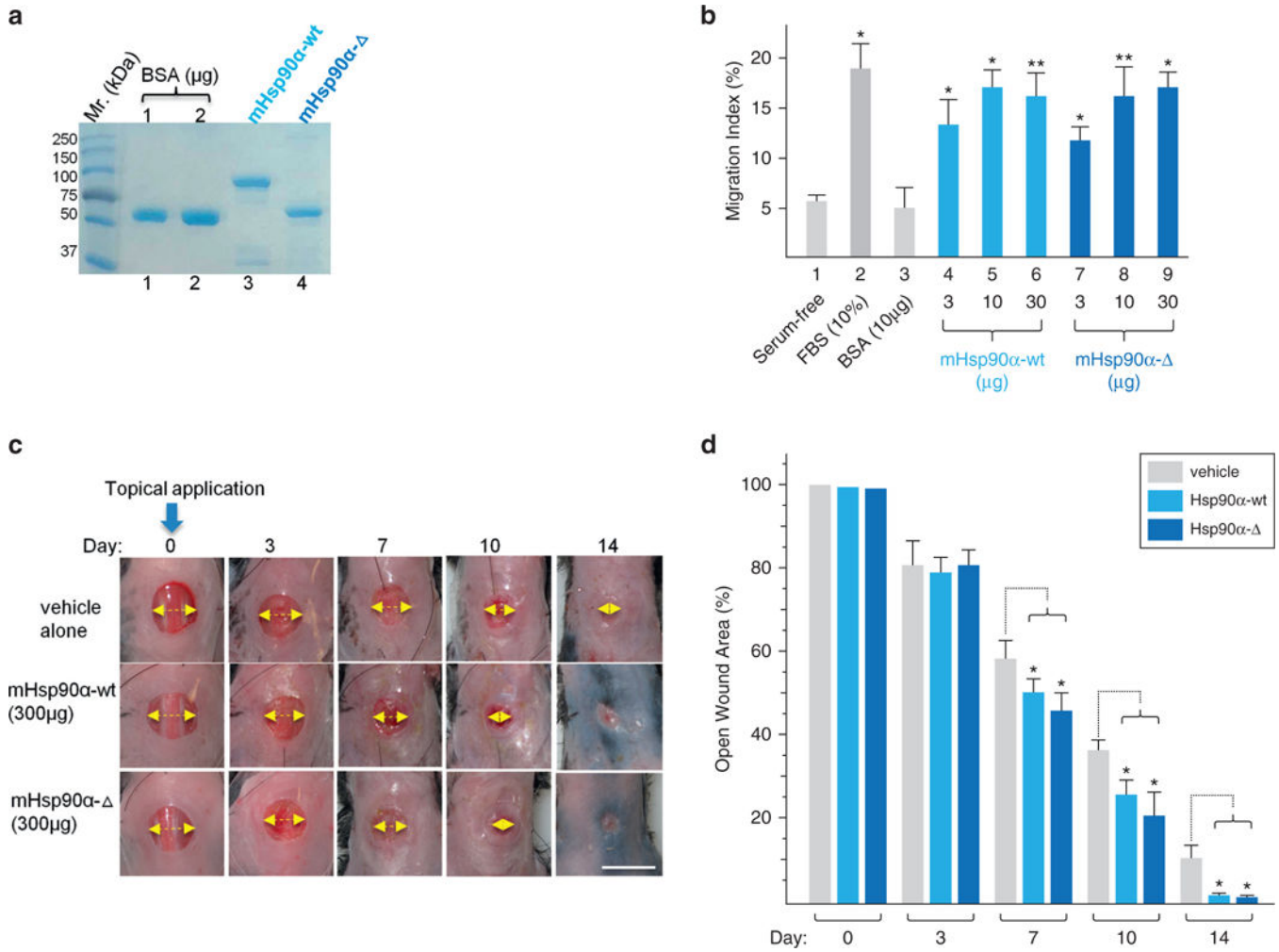

Figure 5. Topically applied recombinant Hsp90α-Δ protein promotes wound closure as effectively as Hsp90α-wt protein.

(**a**) Recombinant mouse Hsp90α-Δ and mouse Hsp90α-wt proteins were produced from cDNAs isolated from the dermal fibroblasts of the mice by pET bacterium inducible expression system, purified by fast protein liquid chromatography and visualized on a Coomassie blue-stained SDS gel. (**b**) Colloidal gold migration assay of human keratinocytes under the indicated stimulations. (**c**) Images of wound closure in Hsp90α-wt mice under carboxymethyl cellulose, Hsp90α-Δ, or Hsp90α-wt protein treatment. The yellow arrow indicates the relative distance of the yet unhealed portion of a wound. (**d**) Quantitation of the triplicate wounds from the experiment shown in (**c**), n = 3. $*P \leq 0.05$. Scale bar = 1.0 cm. FBS, fetal bovine serum; Hsp, heat shock protein; wt, wild type.

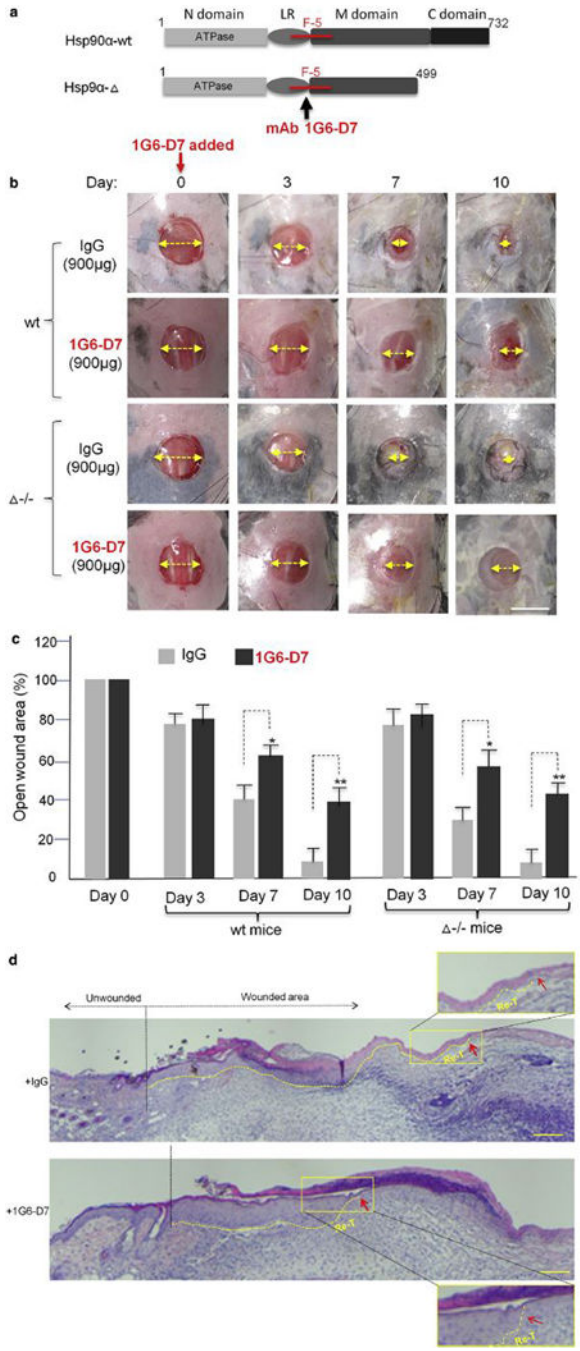

Figure 6. Extracellular Hsp90α-Δ protein is essential for on-time normal wound closure.

(**a**) Schematic presentation of mAb 1G6-D7 binding to fragment-5 region in Hsp90α. (**b**) Effect of topically applied 1G6-D7 on wound closure in Hsp90α-wt and Hsp90α-$\Delta^{-/-}$ mice with a nonspecific mouse IgG as control. The yellow arrow indicates the relative distance of the unhealed portion of a wound. (**c**) Quantitation of triplicate wounds from the experiment shown in (**b**). $*P \leq 0.05$, $**P \leq 0.01$. (**d**) H&E analysis of the wounds on day 7. Fifteen independent images under each condition were analyzed and the representative results a consensus from multiple biopsy sections are presented. Close-up insets show the tips of the

newly re-epithelialized tongue (Re-T). The red arrows point out re-epithelialization. Scale bar for (**b**) = 1.0 cm and for (**d**) = 0.5 mm. Hsp, heat shock protein.